

## Large Effect of a Small Substitution: Competition of Dehydration with Charge Retention and Coulomb Explosion in Gaseous $[(\text{bipy}^{\text{R}})\text{Au}(\mu\text{-O})_2\text{Au}(\text{bipy}^{\text{R}})]^{2+}$ Dications

Eric C. Tyo,<sup>†,‡</sup> A. W. Castleman, Jr.,<sup>†</sup> Detlef Schröder,<sup>\*,‡</sup> Petr Milko,<sup>‡</sup>  
Jana Roithova,<sup>‡,§</sup> Jean Michel Ortega,<sup>||</sup> Maria Agostina Cinellu,<sup>⊥</sup> Fabio Cocco,<sup>⊥</sup> and  
Giovanni Minghetti<sup>⊥</sup>

*Departments of Chemistry and Physics, Pennsylvania State University, University Park, Pennsylvania 16802, Institute of Organic Chemistry and Biochemistry, Flemingovo nám. 2, 16610 Prague 6, Czech Republic, Department of Organic Chemistry, Faculty of Sciences, Charles University in Prague, Hlavova 8, 12843 Prague 2, Czech Republic, Laboratoire Chimie-Physique, Faculté des sciences, UMR8000, CNRS, Université Paris-Sud, Bât. 350, 91405 Orsay, France, and Dipartimento di Chimica, Università di Sassari, Via Vienna 2, I-07100 Sassari, Italy*

Received April 7, 2009; E-mail: Detlef.Schroeder@uochb.cas.cz

**Abstract:** Dinuclear gold(III) clusters with a rhombic  $\text{Au}_2\text{O}_2$  core and 2,2'-bipyridyl ligands substituted in the 6-position ( $\text{bipy}^{\text{R}}$ ) are examined by tandem mass spectrometry. Electrospray ionization of the hexafluorophosphate salts affords the complexes  $[(\text{bipy}^{\text{R}})\text{Au}(\mu\text{-O})_2\text{Au}(\text{bipy}^{\text{R}})]^{2+}$  as free dications in the gas phase. The fragmentation behavior of the mass-selected dications is probed by means of collision-induced dissociation experiments which reveal an exceptionally pronounced effect of substitution. Thus, for the parent compound with  $\text{R} = \text{H}$ , i.e.,  $[(\text{bipy})\text{Au}(\mu\text{-O})_2\text{Au}(\text{bipy})]^{2+}$ , fragmentation at the dicationic stage prevails to result in a loss of neutral  $\text{H}_2\text{O}$  concomitant with an assumed rollover cyclometalation of the bipyridine ligands. In marked contrast, all complexes with alkyl substituents in the 6-position of the ligands ( $\text{bipy}^{\text{R}}$  with  $\text{R} = \text{CH}_3$ ,  $\text{CH}(\text{CH}_3)_2$ ,  $\text{CH}_2\text{C}(\text{CH}_3)_3$ , and  $2,6\text{-C}_6\text{H}_3(\text{CH}_3)_2$ ) as well as the corresponding complex with 6,6'-dimethyl-2,2'-dipyridyl as a ligand exclusively undergo Coulomb explosion to produce two monocationic fragments. It is proposed that the additional steric strain introduced to the central  $\text{Au}_2\text{O}_2$  core by the substituents on the bipyridine ligand, in conjunction with the presence of oxidizable C–H bonds in the substituents, crucially affects the subtle balance between dication dissociation under maintenance of the 2-fold charge and Coulomb explosion into two singly charged fragments.

### Introduction

The chemistry of transition-metal oxo complexes<sup>1</sup> has been of interest to chemists for many years due to their involvement in biological and/or biomimetic oxidations.<sup>2</sup> Particular attention has been devoted in recent years to the oxo complexes of late transition metals (groups 9–11),<sup>3</sup> which serve as intermediates in a variety of oxygen-based processes. For example, they could be involved in reactions promoted by copper-containing enzymes,<sup>4</sup> in catalytic converter processes,<sup>5</sup> in fuel-cell cathodes,<sup>6</sup> and in industrial oxidation reactions based on noble-metal

catalysts (such as Pd, Pt, Ag, and Au) on solid supports.<sup>7</sup> Moreover, late-transition-metal oxo, as well as hydroxo and aquo, complexes are regarded as potential candidates for application toward artificial photosynthesis and water splitting, a topic of intense global research.<sup>3b,8</sup>

<sup>†</sup> Pennsylvania State University.

<sup>‡</sup> Institute of Organic Chemistry and Biochemistry.

<sup>§</sup> Charles University in Prague.

<sup>||</sup> Université Paris-Sud.

<sup>⊥</sup> Università di Sassari.

- (1) (a) Griffith, W. P. *Coord. Chem. Rev.* **1970**, *5*, 459. (b) Bottomley, F.; Sutin, L. *Adv. Organomet. Chem.* **1988**, *28*, 339. (c) West, B. O. *Polyhedron* **1989**, *8*, 219.
- (2) Meunier, B. *Metal–Oxo and Metal–Peroxo Species in Catalytic Oxidations*; Springer: Berlin, 2000. (b) *Biomimetic Oxidations Catalyzed by Transition Metal Complexes*; Meunier, B., Ed.; Imperial College Press: London, 2000. (c) *High-Valent Iron Intermediates in Biology*; *J. Inorg. Biochem.* **2006**, *100*, 419–880.
- (3) (a) Sharp, P. R. *Comments Inorg. Chem.* **1999**, *21*, 85. (b) Sharp, P. R. *J. Chem. Soc., Dalton Trans.* **2000**, 2647.

- (4) Selected reviews and papers: (a) Holland, P. L.; Tolman, W. B. *Coord. Chem. Rev.* **1999**, *855*, 190–192. (b) Que, L., Jr.; Tolman, W. B. *Angew. Chem., Int. Ed.* **2002**, *41*, 1114. (c) Mirica, M. L.; Ottenwaelder, X.; Stack, T. D. P. *Chem. Rev.* **2004**, *104*, 1013. (d) Lewis, A. E.; Tolman, W. B. *Chem. Rev.* **2004**, *104*, 1047. (e) Shimokawa, C.; Teraoka, J.; Tachi, Y.; Itoh, S. *J. Inorg. Biochem.* **2006**, *100*, 1118. (f) Yoshizawa, K.; Kihama, N.; Kamada, T.; Shiota, Y. *Inorg. Chem.* **2006**, *45*, 3034. (g) Kajita, Y.; Arii, H.; Saito, T.; Nagatomo, S.; Kitagawa, T.; Funahashi, Y.; Ozawa, T.; Masuda, H. *Inorg. Chem.* **2007**, *46*, 3322.
- (5) (a) Shelef, M. *Chem. Rev.* **1995**, *95*, 209. (b) Johnson, G. E.; Mitrić, R.; Tyo, E. C.; Bonačić-Koutecký, V.; Castleman, A. W., Jr. *J. Am. Chem. Soc.* **2008**, *122*, 13912.
- (6) (a) Appleby, A. J.; Foulkes, F. R. *Fuel Cell Handbook*; Krieger Publishing Co.: Malabar, FL, 1993. (b) Somorjai, G. A. *Introduction to Surface Chemistry and Catalysis*; Wiley: New York, 1994. (c) Deluga, G. A.; Salge, J. R.; Schmidt, L. D.; Verykios, X. E. *Science* **2004**, *303*, 993. (d) Kim, W. B.; Voitl, T.; Rodriguez-Rivera, G. J.; Dumesic, J. A. *Science* **2004**, *305*, 1280. (e) Landon, P.; Ferguson, J.; Solsona, B. E.; Garcia, T.; Carley, A. F.; Herzing, A. A.; Kiely, C. J.; Golunskic, S. E.; Hutchings, G. J. *Chem. Commun.* **2005**, 3385.

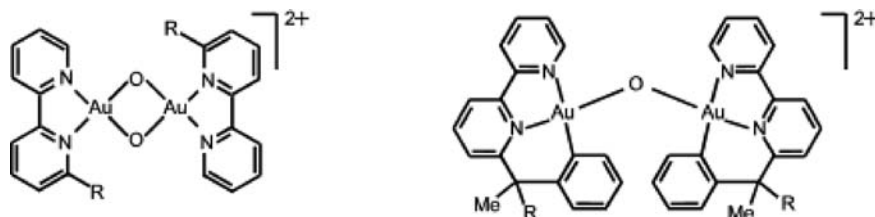
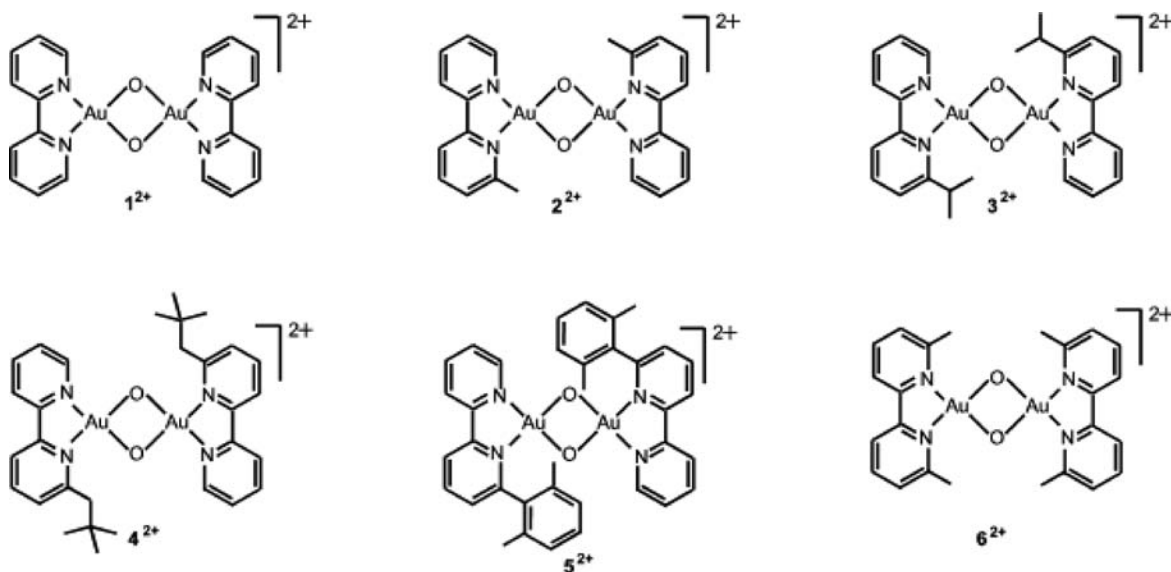
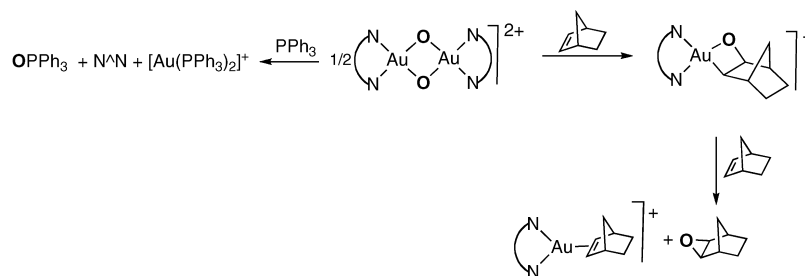
Although intrinsically unstable,<sup>1</sup> a variety of late-transition-metal oxo complexes have been isolated and characterized.<sup>3</sup> The O<sup>2-</sup> unit behaves, most commonly, as a bridging ligand between two or more metal atoms, as found, for example, in some structurally characterized Ni(II),<sup>9</sup> Ni(III),<sup>10</sup> Pd(II),<sup>11</sup> Pt(II),<sup>12</sup> Cu(III),<sup>13</sup> and Au(III)<sup>14</sup> derivatives. Very recently, terminal late-transition-metal oxo complexes, once thought improbable if not impossible to make, have been not only isolated but also authenticated by X-ray diffraction analyses, complemented, in some cases, by various spectroscopic, physical, and chemical methods.<sup>15</sup>

Effectively, oxo complexes of late transition metals have proven to be valuable models providing significant mechanistic insights into oxidation reactions occurring in biological systems as well as in industrial processes. For these purposes, systems containing [M<sub>2</sub>(μ-O)<sub>2</sub>]<sup>n+</sup> cores, in particular those with M = Cu,<sup>4,13</sup> have received considerable attention, and their reactivity has been extensively studied. The copper derivatives contain Cu(III) ions bound to oxo groups and are supported by nitrogen-donor ligands which modulate their reactivity often in subtle ways. They exhibit electrophilic character<sup>4d</sup> and manifest a high propensity to abstract hydrogen atoms from ligand substituents, resulting in *N*-dealkylation reaction,<sup>13a–d,i,16</sup> or from exogenous reagents such as phenols.<sup>17</sup> Oxo transfers to thioethers<sup>18</sup> and phosphines<sup>19</sup> have also been observed. An electrophilic character of the oxo groups in [M<sub>2</sub>(μ-O)<sub>2</sub>]<sup>n+</sup> cores is also displayed by complexes with M = Ni, Co, and Fe.<sup>4b,10a,b,20</sup> In marked contrast, platinum(II) oxo groups act as Brønsted bases and nucleophiles: they can be protonated or methylated to give hydroxo- and methoxo-bridged derivatives, respectively, and associate with a variety of [L<sub>m</sub>M']<sup>n+</sup> fragments, e.g., (PPh<sub>3</sub>)Au<sup>+3,9</sup>

Several years ago, some of us reported the synthesis of two series of gold(III) oxo-bridged complexes, namely, [(N<sup>^</sup>N)Au(μ-O)<sub>2</sub>Au(N<sup>^</sup>N)]<sup>2+</sup> [N<sup>^</sup>N = 6-alkyl-2,2'-bipyridine<sup>14a</sup> and 2,2'-bipyridine<sup>14c</sup>] and [(C<sup>^</sup>N<sup>^</sup>N)Au(μ-O)Au(C<sup>^</sup>N<sup>^</sup>N)]<sup>2+</sup> (HC<sup>^</sup>N<sup>^</sup>N = 6-benzyl-2,2'-bipyridine)<sup>14b</sup> (Chart 1), by hydrolysis reaction of the corresponding mononuclear chlorides. In general, these [(N<sup>^</sup>N)Au(μ-O)<sub>2</sub>Au(N<sup>^</sup>N)]<sup>2+</sup> derivatives (Chart 2) feature a Au<sub>2</sub>O<sub>2</sub> “diamond core” linked to two bipyridine ligands in a roughly planar arrangement and short (from 2.96 to 3.04 Å) Au...Au distances; the Au–O distances, in the range 1.96–1.98

- (7) (a) Boring, E.; Geletii, Y.; Hill, C. L. In *Catalytic Activation of Dioxygen*; Simandi, L. L., Ed.; Kluwer: Dordrecht, The Netherlands, 2001. (b) *Catalysis by Gold*; Hutchings, G. J., Haruta, M., Eds.; Elsevier: New York, 2005; Vol. 291. (c) Neumann, R. In *Transition Metals for Organic Synthesis*, 2nd ed.; Beller, M., Bolm, C., Eds.; Wiley-VCH: Weinheim, Germany, 2004; Vol. 2, p 415. (d) Della Pina, C.; Falletta, E.; Prati, L.; Rossi, M. *Chem. Soc. Rev.* **2008**, *37*, 2077. (e) Liu, X.; Madix, R. J.; Friend, C. M. *Chem. Soc. Rev.* **2008**, *37*, 2243. (f) Hutchings, G. J. *Chem. Soc. Rev.* **2008**, *37*, 5523. (g) Johnson, G. E.; Reilly, N. M.; Tyo, E. C.; Castleman, A. W., Jr. *J. Phys. Chem. C* **2008**, *112*, 9730. (h) Bürgel, C.; Reilly, N. M.; Johnson, G. E.; Mitrić, R.; Kimble, M. L.; Castleman, A. W., Jr.; Bonačić-Koutecký, V. *J. Am. Chem. Soc.* **2008**, *130*, 1694.
- (8) (a) Ruettinger, W.; Dismukes, G. C. *Chem. Rev.* **1997**, *97*, 1. (b) Yagi, M.; Kaneko, M. *Chem. Rev.* **2001**, *101*, 21. (c) Alstrum-Acevedo, J. H.; Brennaman, M. K.; Meyer, T. J. *Inorg. Chem.* **2005**, *44*, 6802. (d) Dempsey, J. L.; Esswein, A. J.; Manke, D. R.; Rosenthal, J.; Soper, J. D.; Nocera, D. G. *Inorg. Chem.* **2005**, *44*, 6879. (e) Lewis, N. S.; Nocera, D. G. *Proc. Natl. Acad. Sci. U.S.A.* **2006**, *103*, 15729. (f) Ozerov, O. V. *Chem. Soc. Rev.* **2009**, *38*, 83.
- (9) Singh, A.; Anandhi, U.; Cinellu, M. A.; Sharp, P. R. *Dalton. Trans.* **2008**, 2314.
- (10) (a) Hikichi, S.; Yoshizawa, M.; Sasakura, Y.; Akita, M.; Moro-oka, Y. *J. Am. Chem. Soc.* **1998**, *120*, 10567. (b) Hikichi, S.; Yoshizawa, M.; Sasakura, Komatsushiki, H.; Moro-oka, Y.; Akita, M. *Chem.–Eur. J.* **2001**, *7*, 5011. (c) Cho, J.; Furutachi, H.; Fujinami, S.; Tosha, T.; Ohtsu, H.; Ikeda, O.; Suzuki, A.; Nomura, M.; Uruga, T.; Tanida, H.; Kawai, T.; Tanaka, K.; Kitagawa, T.; Suzuki, M. *Inorg. Chem.* **2006**, *45*, 2873.
- (11) (a) Zhang, Y.; Puddephatt, R. J.; Manojlovic-Muir, L.; Muir, K. W. *Chem. Commun.* **1996**, 2599. (b) Singh, A.; Sharp, P. R. *Dalton. Trans.* **2005**, 2080.
- (12) (a) Longato, B.; Bandoli, G.; Dolmella, A. *Eur. J. Inorg. Chem.* **2004**, 1092. (b) Li, W.; Barnes, C. L.; Sharp, P. R. *J. Chem. Soc., Chem. Commun.* **1990**, 1634. (c) Li, J. J.; Sharp, P. R. *Inorg. Chem.* **1994**, *33*, 183. (d) Li, J. J.; Li, W.; Sharp, P. R. *Inorg. Chem.* **1996**, *35*, 604. (e) Shan, H.; Sharp, P. R. *Inorg. Chem.* **1998**, *37*, 5727. (f) Singh, A.; Sharp, P. R. *Organometallics* **2006**, *25*, 678.
- (13) (a) Mahapatra, S.; Halfen, J.; Wilkinson, E.; Pan, G.; Cramer, C. J.; Que, L., Jr.; Tolman, W. B. *J. Am. Chem. Soc.* **1995**, *117*, 8865. (b) Halfen, J. A.; Mahapatra, S.; Wilkinson, E. C.; Kaderli, S.; Young, V. G.; Que, L., Jr.; Zuberbühler, A. D.; Tolman, W. B. *Science* **1996**, *271*, 1397. (c) Mahapatra, S.; Halfen, J. A.; Wilkinson, E. C.; Pan, G. F.; Wang, X. D.; Young, V. G.; Cramer, C. J.; Que, L., Jr.; Tolman, W. B. *J. Am. Chem. Soc.* **1996**, *118*, 11555. (d) Mahadevan, V.; Hou, Z. G.; Cole, A. P.; Root, D. E.; Lal, T. K.; Solomon, E. I.; Stack, T. D. P. *J. Am. Chem. Soc.* **1997**, *119*, 11996. (e) Mahapatra, S.; Young, V. G.; Kaderli, S.; Zuberbühler, A. D.; Tolman, W. B. *Angew. Chem., Int. Ed. Engl.* **1997**, *36*, 130. (f) Hayashi, H.; Fujinami, S.; Nagatomo, S.; Ogo, S.; Suzuki, M.; Uehara, A.; Watanabe, Y.; Kitagawa, T. *J. Am. Chem. Soc.* **2000**, *122*, 2124. (g) Straub, B. F.; Rominger, F.; Hofmann, P. *Chem. Commun.* **2000**, 1611. (h) Aboelella, N. W.; Lewis, E. A.; Reynolds, A. M.; Brennessel, W. W.; Cramer, C. J.; Tolman, W. B. *J. Am. Chem. Soc.* **2002**, *124*, 10660. (i) Cole, A. P.; Mahadevan, V.; Mirica, L. M.; Ottenwaelder, X.; Stack, T. D. P. *Inorg. Chem.* **2005**, *44*, 7345–7364, and references therein.
- (14) (a) Cinellu, M. A.; Minghetti, G.; Pinna, M. V.; Stoccoro, S.; Zucca, A.; Manassero, M.; Sansoni, M. *J. Chem. Soc., Dalton Trans.* **1998**, 1735. (b) Cinellu, M. A.; Minghetti, G.; Pinna, M. V.; Stoccoro, S.; Zucca, A.; Manassero, M. *Chem. Commun.* **1998**, 2397. (c) Cinellu, M. A.; Minghetti, G.; Pinna, M. V.; Stoccoro, S.; Zucca, A.; Manassero, M. *J. Chem. Soc., Dalton Trans.* **2000**, 1261. (d) Gabbiani, C.; Casini, A.; Messori, L.; Guerri, A.; Cinellu, M. A.; Minghetti, G.; Corsini, M.; Rosani, C.; Zanello, P.; Arca, M. *Inorg. Chem.* **2008**, *47*, 2368.
- (15) Ir(V): (a) Hay-Motherwell, R. S.; Wilkinson, G.; Hussain-Bates, B.; Hursthouse, M. B. *Polyhedron* **1993**, *12*, 2009. Pd(IV): (b) Anderson, T. M.; Cao, R.; Slonkina, E.; Hedman, B.; Hodgson, K. O.; Hardcastle, K. I.; Neiwert, W. A.; Wu, S.; Kirk, M. L.; Knottenbelt, S.; Depperman, E. C.; Keita, B.; Nadjo, L.; Musaev, D. G.; Morokuma, K.; Hill, C. L. *J. Am. Chem. Soc.* **2005**, *127*, 11948. Pt(IV): (c) Anderson, T. M.; Neiwert, W. A.; Kirk, M. L.; Piccoli, P. M. B.; Schultz, A. J.; Koetzle, T. F.; Musaev, D. G.; Morokuma, K.; Cao, R.; Hill, C. L. *Science* **2004**, *306*, 2074. (d) Poverenov, E.; Efreimenko, I.; Frenkel, A. I.; Ben-David, Y.; Shimoni, L. J. W.; Leitus, G.; Konstantinovskii, L.; Martin, J. M. L.; Milstein, D. *Nature* **2008**, *455*, 1093. Ag(III): (e) Shu-Yan, Y.; Meng-Chang, S. *Inorg. Chem.* **1994**, *33*, 1251. Au(III): (f) Cao, R.; Anderson, T. M.; Piccoli, P. M. B.; Schultz, A. J.; Koetzle, T. F.; Geletii, Y. V.; Slonkina, E.; Hedman, B.; Hodgson, K. O.; Hardcastle, K. I.; Fang, X.; Kirk, M. L.; Knottenbelt, S.; Kögerler, P.; Musaev, D. G.; Morokuma, K.; Takahashi, M.; Hill, C. L. *J. Am. Chem. Soc.* **2007**, *129*, 11118.
- (16) See also: (a) Mahapatra, S.; Halfen, J. A.; Tolman, W. B. *J. Am. Chem. Soc.* **1996**, *118*, 11575. (b) Cramer, C. J.; Pak, Y. *Theor. Chem. Acc.* **2001**, *105*, 477. (c) Cramer, C. J.; Kinsinger, C. R.; Pak, Y. *THEOCHEM* **2003**, *632*, 111. (d) Kajita, Y.; Arii, H.; Saito, T.; Saito, Y.; Nagatomo, S.; Kitagawa, T.; Funahashi, Y.; Ozawa, T.; Masuda, H. *Inorg. Chem.* **2007**, *46*, 3322.
- (17) Some selected papers: (a) Mahadevan, V.; DuBois, J. L.; Hedman, B.; Hodgson, K. O.; Stack, T. D. P. *J. Am. Chem. Soc.* **1999**, *121*, 5583. (b) Osako, T.; Ohkubo, K.; Taki, M.; Tachi, Y.; Fukuzumi, S.; Itoh, S. *J. Am. Chem. Soc.* **2003**, *125*, 11027. (c) Shearer, J.; Zhang, C. X.; Zakharov, L. N.; Rheingold, A. L.; Karlin, K. D. *J. Am. Chem. Soc.* **2005**, *127*, 5469.
- (18) Taki, M.; Itoh, S.; Fukuzumi, S. *J. Am. Chem. Soc.* **2002**, *124*, 998.
- (19) Mahadevan, V.; Henson, M. J.; Solomon, E. I.; Stack, T. D. P. *J. Am. Chem. Soc.* **2000**, *122*, 10249.
- (20) (a) Shiren, K.; Ogo, S.; Fujinami, S.; Hayashi, H.; Suzuki, M.; Uehara, A.; Watanabe, Y.; Moro-oka, Y. *J. Am. Chem. Soc.* **2000**, *122*, 254. (b) Mandimutsira, B. S.; Yamarik, J. L.; Brunold, T. C.; Gu, W.; Cramer, S. P.; Riordan, C. G. *J. Am. Chem. Soc.* **2001**, *123*, 9194. (c) Schenker, R.; Mandimutsira, B. S.; Riordan, C. G.; Brunold, T. C. *J. Am. Chem. Soc.* **2002**, *124*, 13842. (d) Itoh, S.; Bandoh, H.; Nakagawa, M.; Nagatomo, S.; Kitagawa, T.; Karlin, K. D.; Fukuzumi, S. *J. Am. Chem. Soc.* **2001**, *123*, 11168. (e) Skulan, A. J.; Hanson, M. A.; Hsu, H.-F.; Que, L., Jr.; Solomon, E. I. *J. Am. Chem. Soc.* **2003**, *125*, 7344.

## Chart 1. Gold(III) Oxo-Bridged Complexes

Chart 2. Structures of the Binuclear Gold Oxo Clusters  $1^{2+}$ – $6^{2+}$ Scheme 1<sup>a</sup>

<sup>a</sup>  $N^N = \text{bipy}^R$  ( $R = \text{Me}, \text{CHMe}_2, \text{CH}_2\text{CMe}_3, (2,6\text{-Me}_2)\text{C}_6\text{H}_3, \text{ or } 6,6'\text{-dimethyl-2,2'-bipyridine}$ ).

Å, are indicative of a single bond.<sup>14a,d</sup> Introduction of different kinds of alkyl or aryl substituents on the 6 (and 6') position(s) of the bipyridine ligand leads to small structural changes, mainly in the Au–N, Au···Au, and O···O distances as well as in the N–Au–O angle facing the substituent in position 6.<sup>14a,d</sup>

These complexes display an interesting chemistry in solution. The 6-substituted 2,2'-bipyridine derivatives  $2^{2+}$ – $6^{2+}$  are able to transfer oxygen atoms to  $\text{PPh}_3$ , to give  $\text{OPPh}_3$ , as well as to olefins, forming oxygenated organic products and gold(I) alkene complexes via auroxacyclobutane intermediates (Scheme 1).<sup>21</sup> For the sake of simplicity, we abbreviate the 6-substituted bipyridine ligands as  $\text{bipy}^R$  in the following.

The complexes  $1^{2+}$ ,  $2^{2+}$ , and  $4^{2+}$ – $6^{2+}$  show appreciable stability under physiological-like conditions and manifest

important antiproliferative effects toward selected human tumor cell lines; they are also able to interact with some model proteins.<sup>22</sup> As for the metrical parameters, differences in substitution were found to change the cytotoxic properties of these compounds. The  $\text{IC}_{50}$  values of complexes  $1^{2+}$ – $5^{2+}$  spread a range of 10–30  $\mu\text{M}$  when acting on a cell line of human ovarian carcinoma, whereas compound  $6^{2+}$  is significantly more effective, having an  $\text{IC}_{50}$  value of ca. 2  $\mu\text{M}$ .<sup>22</sup> Important correlations have emerged among the cytotoxic potency, oxidizing power, and structural parameters of these complexes. In particular, complex  $6^{2+}$ , which shows the largest structural deviations with respect to the parent compound  $1^{2+}$ , also features the highest oxidizing power, the least thermal stability, and the greatest cytotoxic activity.<sup>14d</sup> This trend could be theoretically reproduced with a good accuracy by means of DFT calculations. In particular, it was established that the observed structural

(21) (a) Cinellu, M. A.; Minghetti, G.; Stoccoro, S.; Zucca, A.; Manassero, M. *Chem. Commun.* **2004**, 1618. (b) Cinellu, M. A.; Minghetti, G.; Cocco, F.; Stoccoro, S.; Zucca, A.; Manassero, M. *Angew. Chem., Int. Ed.* **2005**, *44*, 6892. (c) Cinellu, M. A.; Minghetti, G.; Cocco, F.; Stoccoro, S.; Zucca, A.; Manassero, M.; Arca, M. *Dalton Trans.* **2006**, 5703.

(22) Casini, A.; Cinellu, M. A.; Minghetti, G.; Gabbiani, C.; Coronello, M.; Mini, E.; Messori, L. *J. Med. Chem.* **2006**, *49*, 5524.

variations are primarily to be ascribed to electronic features rather than to solid-state effects.<sup>14d</sup>

In this work, we perform tandem mass spectrometric analysis, which is an approach complementary to the condensed-phase studies, to investigate the properties of the compounds shown in Chart 1, in particular the dissociation characteristic of the free dicationic complexes  $1^{2+}$ – $6^{2+}$  are probed. To this end, the bulk complexes are transferred to the gaseous phase by means of electrospray ionization (ESI) and the dications generated are characterized by collision-induced dissociation (CID) experiments with the aim to determine possible relationships between the fragmentation patterns and the bonding characteristics. Moreover, as metal oxide species, the  $[(\text{bipy}^R)\text{Au}(\mu\text{-O})_2\text{Au}(\text{bipy}^R)]^{2+}$  dications may potentially serve as oxidants for the activation of hydrocarbons and related substrates in the gas phase, which is a subject of intense research.<sup>23</sup> A further motivation of interest arises from the fact that the title compounds are relatively small multiply charged ions, and thus, several fundamental questions emerge about the stability of the isolated dications in the gas phase as well as their chemical reactivity.<sup>24–26</sup>

### Experimental and Theoretical Methods

The experiments were performed with a TSQ Classic mass spectrometer which has been described previously.<sup>27</sup> Briefly, the TSQ Classic consists of an ESI source combined with a tandem mass spectrometer of QQQ configuration (Q stands for quadrupole and O for octopole). The investigated ions were generated by ESI of dilute methanolic solutions of bis(hexafluorophosphate)s of  $1^{2+}$ – $6^{2+}$  at a flow rate of  $5 \mu\text{L}\cdot\text{min}^{-1}$ , and the transfer capillary was kept at 200 °C. The first quadrupole was used to mass scan the spectrum of the ions formed upon ESI or to select the ions of interest. For CID, the mass-selected ions were guided through the octopole serving as a collision chamber followed by mass analysis of the ionic reaction products by means of the second quadrupole and subsequent detection. Xenon was used as a collision gas at a typical pressure of  $(0.3\text{--}2) \times 10^{-4}$  mbar, where the lower border of this range corresponds to approximate single-collision conditions.<sup>28</sup> Using a previously described approximate method based on sigmoid functions of the type  $I_i(E_{\text{CM}}) = (\text{BR}_i)/(1 + e^{(E_{1/2} - E_{\text{CM}})/b_i})$ ,<sup>29,30</sup> phenomenological appearance energies (AEs) are derived from the

energy dependences of the product distributions in the CID spectra. Here,  $\text{BR}_i$  stands for the branching ratio of a particular product ion ( $\sum \text{BR}_i = 1$ ),  $E_{1/2}$  is the energy at which the sigmoid function has reached half of its maximum,  $E_{\text{CM}}$  is the collision energy in the center-of-mass frame ( $E_{\text{CM}} = z m_T/(m_T + m_i) E_{\text{lab}}$ , where  $z$  is the ion's charge and  $m_T$  and  $m_i$  stand for the masses of the collision gas and the ion, respectively), and  $b$  ( $\text{eV}^{-1}$ ) describes the rise of the sigmoid curve and thus the phenomenological energy dependence. We note, however, that, for the heavyweight molecular dications under study, entropic effects and also kinetic shifts in ion dissociation will be of utmost importance.<sup>31</sup> The appearance energies given below should thus only be considered as semiquantitative measures for the fragmentation behavior of the homologous complexes studied in this work. While the empirical fit using sigmoid functions is able to reproduce the measured ion yields,<sup>32</sup> it is obvious that neither  $E_{1/2}$  nor AE corresponds to the intrinsic thermochemistry of the fragmentation of interest.<sup>31</sup>

A few additional measurements were performed with a Finnigan LCQ Classic ion-trap mass spectrometer which has been described elsewhere.<sup>33</sup> In brief the LCQ bears a conventional ESI source consisting of the spray unit (typical flow rate  $5 \mu\text{L}/\text{min}$ , typical spray voltage 5 kV) with nitrogen as a sheath gas, followed by a heated transfer capillary (kept at 200 °C), a first set of lenses which determine the softness or hardness of ionization by variation of the degree of collisional activation in the medium-pressure regime,<sup>34,35</sup> two transfer octopoles, and a Paul ion trap with ca.  $10^{-3}$  mbar helium for ion storage and manipulation including a variety of  $\text{MS}^n$  experiments.<sup>36</sup> For detection, the ions are ejected from the trap to an electron multiplier. Due to limitations of the differential pumping system and the relatively short distance (ca. 30 cm) of the ion trap from the spray needle, considerable amounts of the spray solvent, nitrogen used as the sheath gas, and residual water are present in the ion trap. As some of the fragment ions rapidly react with these reagents, the interpretation of the  $\text{MS}/\text{MS}$  spectra is rendered more difficult, but we have chosen the LCQ because it allows  $\text{MS}^n$  experiments with proper mass selection of all intermediates; note that rapid ion/molecule reactions can even prevent the detection of reactive species in an ion trap.<sup>37</sup> Low-energy CID was performed by application of an excitation ac voltage to the end caps of the trap to induce collisions of the isolated ions with the helium buffer gas for a period of 10 ms. While the CID energies can be varied continuously and also schemes for the conversion into threshold energies have been proposed,<sup>38</sup> we refrain

- (23) (a) Schröder, D.; Schwarz, H. *Angew. Chem., Int. Ed. Engl.* **1995**, *34*, 1973. (b) Schröder, D.; Shaik, S.; Schwarz, H. *Struct. Bonding (Berlin)* **2000**, *97*, 91. (c) Schröder, D.; Schwarz, H. *Top. Organomet. Chem.* **2007**, *22*, 1. (d) Schröder, D.; Schwarz, H. *Proc. Natl. Acad. Sci. (U.S.A.)* **2008**, *105*, 18114.
- (24) (a) Schröder, D.; Schwarz, H. *J. Phys. Chem. A* **1999**, *103*, 7385. (b) Schröder, D. *Angew. Chem., Int. Ed.* **2004**, *43*, 1329.
- (25) (a) Price, S. D. *Phys. Chem. Chem. Phys.* **2003**, *5*, 1717. (b) Price, S. D. *Int. J. Mass Spectrom.* **2006**, *260*, 1.
- (26) Roithová, J.; Schröder, D. *Phys. Chem. Chem. Phys.* **2007**, *9*, 2341.
- (27) (a) Roithová, J.; Schröder, D. *Phys. Chem. Chem. Phys.* **2007**, *9*, 713. (b) Roithová, J.; Schröder, D.; Mišek, J.; Stara, I. G.; Starý, I. *J. Mass Spectrom.* **2007**, *42*, 1233.
- (28) Schröder, D.; Weiske, T.; Schwarz, H. *Int. J. Mass Spectrom.* **2002**, *219*, 729.
- (29) The conception to use sigmoid functions for modeling of the energy-dependent CID data goes back to the shape of photoionization breakdown curves (ref 29a) and the thermokinetic method of Bouchoux et al. (ref 29b). While the approach is purely phenomenological, it requires a minimal set of parameters and no additional assumptions and can directly be applied to the raw data. The major conceptual advantage is of scholarly nature, however, as this simple formalism allows a qualitative description of the energy behavior of a set of compounds with a few parameters, i.e.,  $E_{1/2}$ ,  $b_{1/2}$ , and the AE derived thereof, and thus permits a comparison of different ions without explicit presentation of all energy-dependent CID data as figures. (a) Baer, T. In *Encyclopedia of Mass Spectrometry*; Armentrout, P. B., Ed.; Elsevier: Amsterdam, 2003; Vol. 1, p 381. (b) Bouchoux, G.; Leblanc, D.; Salpin, J. Y. *Int. J. Mass Spectrom.* **1996**, *153*, 37.

- (30) Schröder, D.; Engeser, M.; Brönstrup, M.; Daniel, C.; Spandl, J.; Hartl, H. *Int. J. Mass Spectrom.* **2003**, *228*, 743.
- (31) (a) Rodgers, M. T.; Armentrout, P. B. *J. Chem. Phys.* **1998**, *109*, 1787. (b) Ervin, K. M. *Chem. Rev.* **2001**, *101*, 391. (c) Rodgers, M. T.; Armentrout, P. B. *Acc. Chem. Res.* **2004**, *37*, 989. (d) Armentrout, P. B.; Ervin, K. M.; Rodgers, M. T. *J. Phys. Chem. A* **2008**, *112*, 10071.
- (32) (a) Schröder, D.; Engeser, M.; Schwarz, H.; Rosenthal, E. C. E.; Döbler, J.; Sauer, J. *Inorg. Chem.* **2006**, *45*, 6235. (b) Trage, C.; Diefenbach, M.; Schröder, D.; Schwarz, H. *Chem.—Eur. J.* **2006**, *12*, 2454. (c) Gruene, P.; Trage, C.; Schröder, D.; Schwarz, H. *Eur. J. Inorg. Chem.* **2006**, *2006*, 4546.
- (33) Tintaru, A.; Roithová, J.; Schröder, D.; Charles, L.; Jušinski, J.; Glasovac, Z.; Eckert-Maksić, M. *J. Phys. Chem.* **2008**, *112*, 12097.
- (34) Cech, N. B.; Enke, C. G. *Mass Spectrom. Rev.* **2001**, *20*, 362.
- (35) (a) Schröder, D.; Weiske, T.; Schwarz, H. *Int. J. Mass Spectrom.* **2002**, *219*, 729. (b) Trage, C.; Diefenbach, M.; Schröder, D.; Schwarz, H. *Chem.—Eur. J.* **2006**, *12*, 2454.
- (36) O'Hair, R. A. J. *Chem. Commun.* **2006**, 1469.
- (37) (a) Jagoda-Cwiklik, B.; Jungwirth, P.; Rulíšek, L.; Milko, P.; Roithová, J.; Lemaire, J.; Maitre, P.; Ortega, J. M.; Schröder, D. *ChemPhysChem* **2007**, *8*, 1629. (b) Milko, P.; Roithová, J.; Schröder, D.; Lemaire, J.; Schwarz, H.; Holthausen, M. C. *Chem.—Eur. J.* **2008**, *14*, 4318.
- (38) (a) Colorado, A.; Brodbelt, J. *J. Am. Soc. Mass Spectrom.* **1996**, *7*, 1116. (b) Waters, T.; O'Hair, R. A. J.; Wedd, A. G. *J. Am. Chem. Soc.* **2003**, *125*, 3384. (c) O'Hair, R. A. J.; Vrkcic, A. K.; James, P. F. *J. Am. Chem. Soc.* **2004**, *126*, 12173. (d) Khairallah, G. N.; O'Hair, R. A. J. *Angew. Chem., Int. Ed.* **2005**, *44*, 728.

from an exact quantification here and rather refer to them as a percentage of the excitation voltage applied.

In addition, gas-phase infrared spectra of the mass-selected dications  $1^{2+}$  and  $2^{2+}$  were recorded with a Bruker Esquire 3000 ion-trap mass spectrometer (IT-MS)<sup>39</sup> mounted to the beamline of a free electron laser at CLIO (Centre Laser Infrarouge Orsay, France). The ions of interest were generated by ESI from methanolic solution as described above and transferred into the ion trap. After mass selection, infrared multiphoton dissociation was induced by admittance of four pulses of IR-laser light to the ion trap, resulting in a total trapping time of about 0.4 s. In the 45 MeV range in which CLIO was operated in these experiments, the IR light covers a spectral range from about 1000 to 1700  $\text{cm}^{-1}$ . Note that, in this kind of action spectra, the assumption that the amount of ion fragmentation is proportional to the IR absorbance is not always justified due to the multiphotonic nature of IRMPD, and the major weight is therefore put on the peak positions, rather than the peak heights, in the IRMPD spectra.<sup>40</sup>

The calculations were performed using the density functional method MPW1PW91<sup>41</sup> in conjunction with the SDD basis sets for gold and 6-311+G(2d,p) basis sets for the other atoms as implemented in the Gaussian 03 suite.<sup>42</sup> For all optimized structures, frequency analyses at the same level of theory were used to assign them as genuine minima or transition structures on the potential-energy surface (PES). All IR spectra given correspond to the singlet states of the studied ions. The triplet state of  $1^{2+}$  lies 1.63 eV above the singlet state, and the triplet state of *trans*- $2^{2+}$  lies 1.58 eV above the corresponding singlet state; therefore, they were not further considered.

## Results and Discussion

This investigation probes the intrinsic properties of a unique set of bare, multiply charged ions and has as its objective a comparison of the fragmentation patterns between members of the series with the structural characteristics and oxidative potential observed in the condensed phase. To this end, the title compounds are dissolved in methanol and are introduced to the gas phase via ESI. Under soft conditions of ionization,<sup>34</sup> ESI of the bis(hexafluorophosphate)s of compounds  $1^{2+}$ – $6^{2+}$  results in mass spectra dominated by the parent dications with few fragments being detected. Adjustment to harsher source conditions results in increasing fragmentation at the expense of the parent dications. Inspection of the isotope patterns confirms the generation of genuine dications for all compounds as revealed by the separation of carbon isotope peaks by 0.5 amu.<sup>43</sup> As these molecular dications are the species of interest for this study, the remainder of the mass spectrum will be disregarded. The collision-induced dissociation (CID) spectra of the mass-selected dicationic gold oxo complexes provide a wealth of information regarding bonding arrangements as well as fragmentation patterns and energetic barriers toward fragmentation at different positions. Furthermore, repulsion between the gold centers of the doubly charged complexes  $2^{2+}$ – $6^{2+}$ , in conjunc-

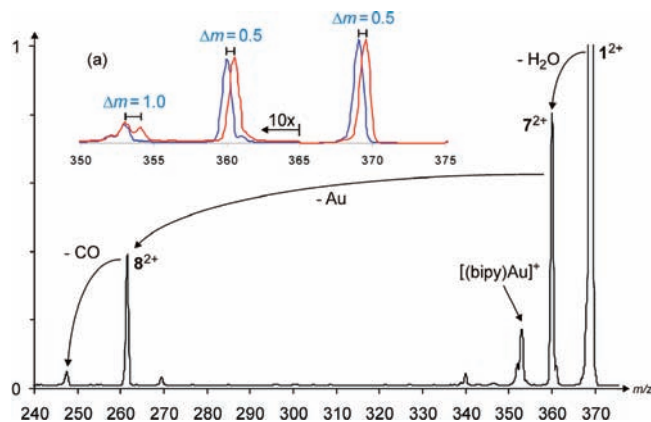


**Figure 1.** Representative CID spectrum of mass-selected  $1^{2+}$  ( $m/z$  369) showing loss of water with maintenance of the 2-fold charge according to reaction 1 and the subsequent dication fragmentations via consecutive expulsions of neutral Au and CO, respectively. The most abundant additional fragment corresponds to the monocationic fragment  $[(bipy)Au]^+$  (reaction 2''); the low-mass region with  $[bipyO - H]^+$  and related fragments (reaction 3) is not shown. Inset a shows the expanded mass regions from  $m/z$  350 to  $m/z$  375 for  $1^{2+}$  ( $m/z$  369.0, blue) and the mass-selected isotope  $[^{13}C]1^{2+}$  ( $m/z$  369.5, red), demonstrating that the loss of  $\Delta m = -16$  amu upon CID of  $1^{2+}$  is due to charge separation according to reaction 2'' without any indication for  $O_2$  loss from the dication with maintenance of the 2-fold charge reaction 2'.

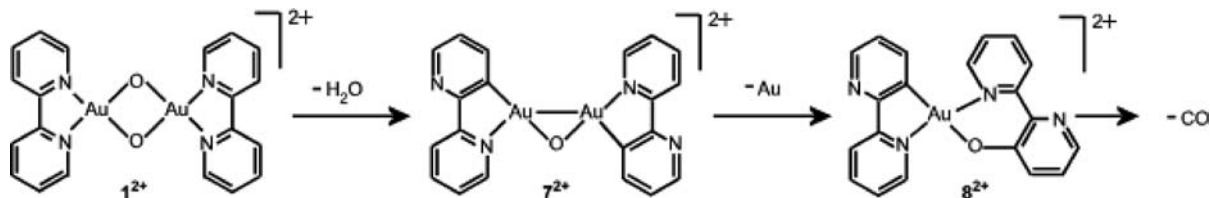
tion with the energy gained in the collision experiment, is sufficient to induce charge separation, thus creating a pair of monocations ("Coulomb explosion").<sup>24–26,44</sup>

**Parent Compound  $1^{2+}$ .** The major dissociation channel upon CID of the parent compound  $1^{2+}$  ( $R = H$ ,  $m/z$  369, Figure 1) corresponds to the loss of neutral water, thus leaving the ionic fragment in the dicationic state (reaction 1). Obviously, reaction 1 involves the loss of two hydrogen atoms from the bipyridyl ligands and one of the bridging oxygen atoms. While the precise position on the bipyridine from which the hydrogen originates cannot be determined through CID, occurrence of a "rollover" cyclometalation<sup>45,46</sup> to form structure  $7^{2+}$  offers a plausible rationale (Scheme 2). Subsequent dissociation of  $7^{2+}$  is observed in which the complex retains the doubly charged state through the loss of a neutral gold atom, thus presumably generating

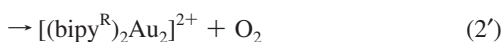
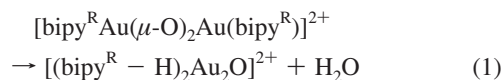
- (39) (a) Mac Aleese, L.; Simon, A.; McMahon, T. B.; Ortega, J. M.; Scuderi, D.; Lemaire, J.; Maitre, P. *Int. J. Mass Spectrom.* **2006**, *249*, 14. (b) Chiavarino, B.; Crestoni, M. E.; Fornarini, S.; Lanucara, F.; Lemaire, J.; Maitre, P. *Angew. Chem., Int. Ed.* **2007**, *46*, 1995. (c) Simon, A.; Aleese, L.; Maitre, P.; Lemaire, J.; McMahon, T. B. *J. Am. Chem. Soc.* **2006**, *129*, 2829.
- (40) Schröder, D.; Schwarz, H.; Milko, P.; Roithová, J. *J. Phys. Chem. A* **2006**, *110*, 8346.
- (41) Adamo, C.; Barone, V. *J. Chem. Phys.* **1998**, *108*, 664.
- (42) *Gaussian 03*, revision C.02; Gaussian, Inc.: Wallingford, CT, 2004.
- (43) See also: (a) Roithová, J.; Milko, P.; Ricketts, C. L.; Schröder, D.; Besson, T.; Dekoj, V.; Bilohradský, M. *J. Am. Chem. Soc.* **2007**, *129*, 10141. (b) Colasson, B.; Save, M.; Renaud, O.; Milko, P.; Roithová, J.; Schröder, D. *Org. Lett.* **2007**, *9*, 4987.

- (44) Folmer, D. E.; Poth, L.; Wisniewski, E. S.; Castleman, A. W., Jr. *Chem. Phys. Lett.* **1998**, *287*, 1.
- (45) (a) Watts, R. J.; Harrington, J. S.; Van Houten, J. *J. Am. Chem. Soc.* **1977**, *99*, 2179. (b) Wickramasinghe, W. A.; Bird, P. H.; Serpone, N. *J. Chem. Soc., Chem. Commun.* **1981**, 1284. (c) Constable, E. C.; Seddon, K. R. *J. Chem. Soc., Chem. Commun.* **1982**, 34. (d) Dholakia, S.; Gillard, R. D.; Wimmer, F. L. *Inorg. Chim. Acta* **1983**, *69*, 179. (e) Nord, G.; Hazell, A. C.; Hazell, R. G.; Farver, O. *Inorg. Chem.* **1983**, *22*, 3429. (f) Spellane, P. J.; Watts, R. J.; Curtis, C. J. *Inorg. Chem.* **1983**, *22*, 4060. (g) Braterman, P. S.; Heath, G. A.; MacKenzie, A. J.; Noble, B. C.; Peacock, R. D.; Yellowlas, L. J. *Inorg. Chem.* **1984**, *23*, 3425. (h) Minghetti, G.; Doppiu, A.; Zucca, A.; Stoccoro, S.; Cinellu, M. A.; Manassero, M.; Sansoni, M. *Chem. Heterocycl. Compd.* **1999**, *8*, 1127. (i) Zucca, A.; Doppiu, A.; Cinellu, M. A.; Stoccoro, S.; Minghetti, G.; Manassero, M. *Organometallics* **2002**, *21*, 783. (j) Minghetti, G.; Stoccoro, S.; Cinellu, M. A.; Soro, B.; Zucca, A. *Organometallics* **2003**, *22*, 4770. (k) Zucca, A.; Cinellu, M. A.; Minghetti, G.; Stoccoro, S.; Manassero, M. *Eur. J. Inorg. Chem.* **2004**, 4484. (l) Stoccoro, S.; Zucca, A.; Petretto, G. L.; Cinellu, M. A.; Minghetti, G.; Manassero, M. *J. Organomet. Chem.* **2006**, *691*, 4135. (m) Minghetti, G.; Stoccoro, S.; Cinellu, M. A.; Petretto, G. L.; Zucca, A. *Organometallics* **2008**, *27*, 3415.
- (46) A rollover metalation of 6,6'-dimethoxy-2,2'-bipyridine has been recently observed in a gold(III) complex: Cocco, F.; Cinellu, M. A.; Minghetti, G.; Maiore, L.; Stoccoro, S.; Zucca, A.; Manassero, M. *Abstract of Papers, XXIII International Conference on Organometallic Chemistry, Rennes, France, July 13–18, 2008*; P550.

**Scheme 2.** Proposed Rollover Cyclometalation of  $1^{2+}$  To Yield the Dication  $7^{2+}$  Concomitant with Neutral Water Loss and the Subsequent Loss of Neutral Gold To Yield the Dication  $8^{2+}$



complex  $8^{2+}$ . The presence of a newly formed C–O bond in  $8^{2+}$  is further supported by the consecutive loss of neutral carbon monoxide, while the fragment still remains in the dication state.



Another fragmentation of the parent compound  $1^{2+}$  by means of cluster cleavage occurring concomitant with a charge separation affords a signal at  $m/z$  353 (thus,  $\Delta m = -16$ ), which could be attributed to three different origins. Charge separation concomitant with transfer of both oxygen atoms to a single gold atom would lead to two monocationic fragments (reaction 2), of which, however, only the signal at  $m/z$  353, corresponding to  $[(\text{bipy})\text{Au}]^+$ , is detected in the case of  $1^{2+}$ . Absence of the second monocationic counterpart at  $m/z$  385, which is denoted as  $[\text{bipy}^{\text{R}}\text{Au}_2\text{O}_2]^+$  in reaction 2 to avoid assignment of a particular structure, might in turn imply that the mass difference of  $\Delta m = -16$  is thus due to a dissociation at the dicationic stage (reaction 2'). An experiment with the natural  $^{13}\text{C}_1$  isotope of  $1^{2+}$  unequivocally demonstrates, however, that  $\Delta m = -16$  is associated with formation of monocationic fragments (see the inset in Figure 1). The signal at  $m/z$  353 is hence assigned to reaction 2'', i.e., Coulomb explosion concomitant with reduction to Au(I) and expulsion of molecular oxygen. As the investigation of the substituted 2,2'-bipyridine derivatives  $2^{2+}$ – $6^{2+}$  sheds more light on this issue, we return to it after having presented further CID data. At elevated collision energies, several organic ions, listed as  $[\text{bipy}^{\text{R}}]^+$  in Table 1, are also formed and are discussed in more detail below. A portion of these ions arise from consecutive dissociations of the fragment ions formed in reactions 1 and 2'', respectively, while some fraction is directly formed from  $1^{2+}$  (reaction 3). However, the data of these minor channels are not analyzed in further detail because the primary fragment  $[(\text{bipy}^{\text{R}} - \text{H})\text{Au}_2\text{O}_2]^+$  formed in reaction 3 consecutively loses neutral gold mono- as well as dioxide<sup>47</sup> and the resulting fragments  $[(\text{bipy}^{\text{R}} - \text{H})\text{AuO}]^+$  and  $[(\text{bipy}^{\text{R}} - \text{H})\text{Au}]^+$  overlap with the much more intense parent ion and  $[(\text{bipy}^{\text{R}})\text{Au}]^+$  formed in reaction 1, respectively.

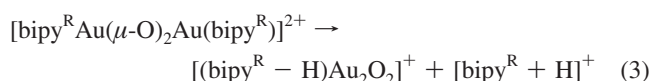


**Table 1.** Major Fragments (Given Relative to the Base Peak Set to 100)<sup>a</sup> in the CID Mass Spectra of the Mass-Selected Dications  $1^{2+}$ – $6^{2+}$  Designated According to the Following Notations: Loss of Neutral Water ( $-\text{H}_2\text{O}$ , Reaction 1), Disproportionation with Oxygen Transfer and Coulomb Explosion ( $\text{O}_{\text{t,CE}}$ , Reaction 2), Disproportionation with Oxygen and Double Hydrogen Atom Transfer as Well as Coulomb Explosion ( $\text{H}_2\text{O}_{\text{t,CE}}$ , Reaction 5), and Formation of Organic Cations Derived from the Bipyridyl Ligand  $[\text{bipy}^{\text{R}}]^+$  (e.g., Reaction 3) and Its Oxygenated Form  $[\text{bipy}^{\text{R}}\text{O}]^+$ <sup>b</sup>

	AE <sup>c</sup>	$E_{1/2}$ <sup>c</sup>	$-\text{H}_2\text{O}$	$\text{O}_{\text{t,CE}}$	$\text{H}_2\text{O}_{\text{t,CE}}$	$[\text{bipy}^{\text{R}}]^+$ <sup>d</sup>	$[\text{bipy}^{\text{R}}\text{O}]^+$ <sup>e</sup>
$1^{2+}$	9.7	14.8	100	20		5	
$2^{2+}$	2.3	5.0	2	100		5	3
$3^{2+}$	0.9	2.7	10	100	65	40	20
$4^{2+}$	1.6	4.1		40	100	50	30
$5^{2+}$	4.2	6.5	1	65	7	100	90
$6^{2+}$	1.7	3.5	>1	100		15	2

<sup>a</sup> The branching ratios given refer to the CID spectra taken at  $E_{1/2}$ .

<sup>b</sup> In addition, the parameter  $E_{1/2}$  resulting from modeling of the CID breakdown graphs with sigmoid functions and the derived phenomenological AEs (both given in electronvolts in the center-of-mass frame) are given. <sup>c</sup> The error of the AE and  $E_{1/2}$  values is conservatively estimated as  $\pm 10\%$ , but at least  $\pm 0.3$  eV. <sup>d</sup> Organic cations derived from the bipyridyl ligands are summarized as  $[\text{bipy}^{\text{R}}]^+$  with the molecular ion  $[\text{bipy}^{\text{R}}]^+$  and the protonated base  $[\text{bipy}^{\text{R}} + \text{H}]^+$  as the major fragments. For the sake of simplicity, the abundances of these fragments are added together in the branching ratios given. <sup>e</sup> Organic cations derived from the oxidized bipyridyl ligands are summarized as  $[\text{bipy}^{\text{R}}\text{O}]^+$  with the cation radical  $[\text{bipy}^{\text{R}}\text{O}]^+$  and  $[\text{bipy}^{\text{R}}\text{O} - \text{H}]^+$  being the major fragments. For the sake of simplicity, the abundances of these fragments are added together in the branching ratios given.

As stated, the major fragmentation channel observed for complex  $1^{2+}$  leads to a compound that remains in the dication state. In contrast, the dications  $2^{2+}$ – $6^{2+}$  (bearing 6-substituted 2,2'-bipyridyl ligands) preferentially undergo Coulomb explosion into monocationic units. This pronounced difference is quite unexpected because all complexes studied contain the same backbone but only differ in hydrocarbon groups attached to their bipyridine units. While the substituents in compounds  $2^{2+}$ – $6^{2+}$  certainly cause a strain in the bonding between the two gold atoms, which lowers the energetic barrier for Coulomb explosion to occur, the observation of largely different preferences in the dissociation pathways is quite astounding. In the condensed phase, introduction of different alkyl or aryl substituents in the 6 (and 6') position(s) of the bipyridine ligand leads to only small structural changes, but bears a dramatic effect on the reactivity and cytotoxic potency of these compounds.<sup>14d,22</sup> A major dissociation channel of the 6-substituted bipyridine derivatives  $2^{2+}$ – $6^{2+}$  corresponds to Coulomb explosion according to reaction 2, resulting in the formation of two monocationic fragments. In this case, both  $\text{Au}(\text{bipy}^{\text{R}})$  units retain a positive charge as they separate; one fragment has both oxygen atoms associated to it, whereas the other is oxygen-deficient.

**6-Methyl Derivative  $2^{2+}$ .** With each complex fragmenting into an oxygen-rich and an oxygen-deficient monocation, equal amounts of both fragment ions should be detected in the mass spectrum. Instead, the CID spectrum of the mass-selected complex  $2^{2+}$  ( $m/z$  383, Figure 2) shows a larger quantity of

(47) Zhai, H. J.; Bürgel, C.; Bonačić-Koutecky, V.; Wang, L. S. *J. Am. Chem. Soc.* **2008**, *130*, 9156.

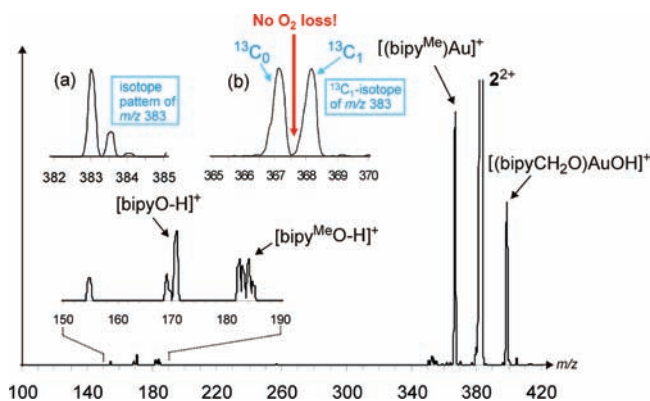


**Figure 2.** CID spectrum of mass-selected  $2^{2+}$  ( $m/z$  383) showing Coulomb explosion according to reaction 2 affording the monocationic fragments  $[(bipy^{Me})Au]^+$  and  $[(bipyCH_2O)AuOH]^+$  as the major products. The low-mass region ( $m/z$  150–190) is also shown as an expanded magnification. Inset a shows the isotope pattern of the parent ion with a characteristic spacing by 0.5 amu. Inset b shows the mass region around  $m/z$  367 in the CID spectrum of mass-selected  $[^{13}C_1]2^{2+}$  ( $m/z$  383.5), which demonstrates that the loss of  $\Delta m = -16$  amu upon CID of  $2^{2+}$  is only due to charge separation according to reaction 2 without any indication for  $O_2$  loss from the dication with maintenance of the 2-fold charge (reaction 2').

oxygen-deficient fragment than expected for a mere Coulomb explosion. The most likely explanation is the parallel occurrence of reaction 2'' already observed in the case of  $1^{2+}$ . Alternatively, loss of molecular oxygen from  $2^{2+}$  (reaction 2') to afford the dicationic cluster  $[(bipy^{Me})_2Au_2]^{2+}$ , which is isobaric with the singly charged, mononuclear cation  $[(bipy^{Me})Au]^+$  would provide a possible rationale. To this end, the natural  $^{13}C_1$  isotope of  $2^{2+}$  ( $m/z$  383.5) was subjected to a CID experiment. For  $[^{13}C_1]2^{2+}$ , loss of neutral  $O_2$  from the dication (reaction 2') would afford a single signal at  $m/z$  367.5, whereas charge separation according to reactions 2 and/or 2'' should afford fragments at  $m/z$  367 and 368 in a 1:1 ratio.<sup>43a</sup> As demonstrated in inset b of Figure 2, only the latter option is detected experimentally; occurrence of reaction 2' can hence be ruled out. Furthermore, a breakdown diagram revealing appearance energies of  $2.3 \pm 0.2$  eV for both major monocation fragments is displayed in Figure 3 and may serve as an example for the energy dependencies discussed further below.

A key question concerns the structure of the fragment ion  $[bipy^R, Au, O_2]^+$  formed in the course of reaction 2, which could correspond to either a genuine dioxygen complex,  $[(bipy^R)Au(O_2)]^+$ , or a gold dioxido cation,  $[(bipy^R)AuO_2]^+$ , both with intact  $bipy^R$  ligands, or a species with an oxygenated ligand. Formation of a gold(III)  $\eta^2$ -peroxo or side-on gold(I) dioxygen complex appears quite conceivable, as these would be analogous to the corresponding complexes of nickel(II), copper(III), rhodium(III), palladium(II), iridium(III), and platinum(II) well-known in solution chemistry.<sup>48</sup> Similarly, such metal peroxo or dioxygen complexes have been characterized in gas-phase experiments, although the isomeric structures of end-on  $M(O_2)^+$  as well as genuine dioxides  $M(O_2)^+$  are also relevant for the isolated species in the gas phase.<sup>49,50</sup> To achieve further understanding of the ion structure, the  $[bipy^{Me}, Au, O_2]^+$  ion was probed by means of CID. While the fragmentation of  $2^{2+}$  to create  $[bipy^{Me}, Au, O_2]^+$  can be achieved in the ESI source under slightly enforced conditions of ionization, irrespective of the conditions applied, the mass-selected ion beam always showed interferences by isobaric complexes containing molecules of

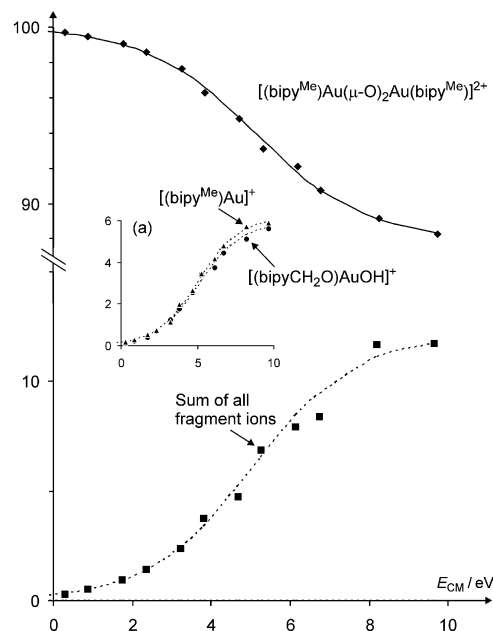


**Figure 3.** CID breakdown diagram of mass-selected  $2^{2+}$  to afford the monocationic fragments  $[(bipy^{Me})Au]^+$  and  $[(bipyCH_2O)AuOH]^+$  as the major products. The lines show the result of fitting a sigmoid function to the experimental abundances of the parent and fragment ions (data points). Inset a shows the energy-dependent fractions of  $[(bipy^{Me})Au]^+$  and  $[(bipyCH_2O)AuOH]^+$ . Note that consecutive fragments are added to the primary dissociation channels; see the text.

methanol used as a solvent. This is particularly unfortunate in the present case because loss of methanol appears at the same mass difference as loss of molecular oxygen (both  $\Delta m = -32$ ), the latter being indicative of a dioxygen complex (reaction 4).



Because the required MS<sup>3</sup> experiment, i.e., generation and mass selection of  $2^{2+}$  and fragmentation and mass selection of

- (48) For some recent examples of  $[L_nM(\eta^2-O_2)]$  complexes in the condensed phase, see the following papers. M = Ni: (a) Fujita, K.; Schenker, R.; Gu, W. W.; Brunold, T. C.; Cramer, S. P.; Riordan, C. G. *Inorg. Chem.* **2004**, *43*, 3324. M = Cu: (b) Pantazis, D. A.; McGrady, J. E. *Inorg. Chem.* **2003**, *42*, 7734. M = Rh: (c) Ahijado, M.; Braun, T.; Noveski, D.; Kochev, N.; Neumann, B.; Stalke, D.; Stämmler, H. G. *Angew. Chem., Int. Ed.* **2005**, *44*, 6947. (d) Tejel, C.; Ciriano, M. A.; Sola, E.; del Rio, M. P.; Rios-Moreno, G.; Laho, F. J.; Oro, L. A. *Angew. Chem., Int. Ed.* **2005**, *44*, 3267. M = Rh, Ir: (e) de Buin, B.; Peters, T. P. J.; Wilting, J. B. M.; Thewissen, S.; Smits, J. M. M.; Gal, A. W. *Eur. J. Inorg. Chem.* **2002**, 2671. M = Pd: (f) Stahl, S.; Thorman, J. L.; Nelson, R. C.; Kozee, M. A. *J. Am. Chem. Soc.* **2001**, *123*, 7188. (g) Stahl, S.; Thorman, J. L.; Nelson, R. C.; Kozee, M. A. *J. Am. Chem. Soc.* **2002**, *124*, 766. M = Pt: (h) Rostovtsev, V. V.; Henling, L. M.; Labinger, J. A.; Bercaw, J. E. *Inorg. Chem.* **2002**, *41*, 3608.
- (49) For gas-phase data on isomeric  $[L_nMO_2]^+$  ions, see the following papers. M = V: (a) Koyanagi, G. K.; Bohme, D. K.; Kretzschmar, I.; Schröder, D.; Schwarz, H. *J. Phys. Chem. A* **2001**, *105*, 4259. M = Cr: (b) Fiedler, A.; Kretzschmar, I.; Schröder, D.; Schwarz, H. *J. Am. Chem. Soc.* **1996**, *118*, 9941. (c) Beyer, M. K.; Berg, C. B.; Achatz, U.; Joos, S.; Niedner-Schatteburg, G.; Bondybej, V. E. *Mol. Phys. Chem.* **2001**, *99*, 699. M = Fe: (d) Schröder, D.; Fiedler, A.; Schwarz, J.; Schwarz, H. *Inorg. Chem.* **1994**, *33*, 5094. M = Ce: (e) Heinemann, C.; Cornehl, H. H.; Schröder, D.; Dolg, M.; Schwarz, H. *Inorg. Chem.* **1996**, *35*, 2463. M = Re: (f) Schröder, D.; Fiedler, A.; Herrmann, W. A.; Schwarz, H. *Angew. Chem., Int. Ed. Engl.* **1995**, *34*, 2517. M = Pt: (g) Brönstrup, M.; Schröder, D.; Kretzschmar, I.; Schwarz, H.; Harvey, J. N. *J. Am. Chem. Soc.* **2001**, *123*, 142.
- (50) For gas-phase data on isomeric  $[(bipy)_2MO_2]^{2+}$  dications with M = Cr, Ru, and Os, see: (a) Molina-Svendsen, H.; Bojesen, G.; McKenzie, C. J. *Inorg. Chem.* **1998**, *37*, 1981. (b) Howe, P. R.; McGrady, J. E.; McKenzie, C. J. *Inorg. Chem.* **2002**, *41*, 2026.

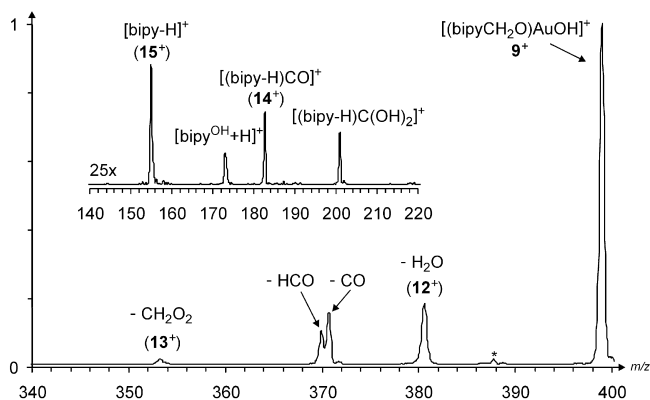


**Figure 4.** CID spectrum of mass-selected  $[\text{bipy}^{\text{Me}},\text{Au},\text{O}_2]^+$  ( $m/z$  399, assigned to structure  $9^+$ ; see the text) generated by CID of mass-selected  $2^{2+}$  ( $m/z$  383) in the ion-trap instrument (see the Experimental and Theoretical Methods). The major fragments correspond to losses of  $\text{H}_2\text{O}$ ,  $\text{CO}$ , and  $\text{CHO}$  with a minor signal due to expulsion of  $\text{CH}_2\text{O}_2$  (most probably  $\text{CO} + \text{H}_2\text{O}$ ). The inset shows the low-mass region where organic ions resulting from oxygenation of the  $\text{bipy}^{\text{Me}}$  ligand appear; the fragment denoted as  $[(\text{bipy} - \text{H})\text{C}(\text{OH})_2]^+$  ( $m/z$  201) results from clustering of the  $[(\text{bipy} - \text{H})\text{CO}]^+$  fragment ( $m/z$  183) with water being present in the trap as a background. The signal at  $m/z$  388 (denoted with an asterisk) and the smaller peak at  $m/z$  389 are due to association of  $m/z$  353 (loss of  $\text{CH}_2\text{O}_2$ ) with  $\text{CD}_3\text{OH}(\text{D})$ , which is used as the spray solvent and diffuses into the ion trap.

$[\text{bipy}^{\text{Me}},\text{Au},\text{O}_2]^+$ , followed by CID and detection, is impossible in a triple-quadrupole instrument, we switched to an ion-trap mass spectrometer as the alternative. An ion trap has no physical limitations of  $n$  in  $\text{MS}^n$  experiments and only requires sufficient ion abundances.<sup>36</sup> A drawback is, however, that the sampling and storage times of ions in a trap are relatively large (minimum of several milliseconds), and meanwhile, the pressure is relatively high ( $10^{-3}$  mbar), compared to microseconds and  $10^{-7}$  mbar in the triple-quadrupole device. As a consequence, at least for reactive metal ions, a significant amount of reactions with background molecules (primarily water and nitrogen) have to be taken into account.<sup>37</sup> Nevertheless, the advantage of a proper mass selection of all intermediates in the  $\text{MS}^n$  sequence outweighs this disadvantage in the present case.

Figure 4 shows a representative CID spectrum of mass-selected  $[\text{bipy}^{\text{Me}},\text{Au},\text{O}_2]^+$ . In the mass region of the parent ion, the major fragments are due to losses of  $\text{H}_2\text{O}$ ,  $\text{CO}$ ,  $\text{HCO}$ , and  $\text{CH}_2\text{O}_2$ , where the latter presumably is a combined loss of water and carbon monoxide. Notably, however, not even a trace of dioxygen loss is apparent in the  $\text{MS}^n$  spectrum, thereby disfavoring the formation of a dioxygen complex. Instead, expulsions of water as well as carbon monoxide demonstrate the occurrence of C–H as well as C–C bond activation of the ligand. Moreover, several organic ions observed in the low-mass region of the spectrum (inset in Figure 4) indicate the formation of new C–O bonds of the  $\text{bipy}^{\text{Me}}$  ligand. Thereby, of the three feasible structural alternatives proposed above for the  $[\text{bipy}^{\text{Me}},\text{Au},\text{O}_2]^+$  fragment, these results very much support the third option, i.e., oxidation of the ligand by the oxygen atoms present in the complex. Even without having performed regio-specific isotope labeling experiments, the drastic change of the fragmentation behavior between the parent compound  $1^{2+}$  and the methyl derivative  $2^{2+}$  suggests an active participation of the substituent. In other words, the Coulomb explosion of  $2^{2+}$  according to reaction 2 is enabled by the occurrence of C–H bond activation of the methyl substituents. A plausible mechanistic scenario, which is consistent with all experimental findings, is proposed in Scheme 3.

Thus, the first step in the fragmentation of  $2^{2+}$  involves activation of a C–H bond present on one of the 6-methyl groups of the  $\text{bipy}^{\text{Me}}$  ligands, followed by cluster cleavage and charge separation to afford the monocations  $9^+$  and  $10^+$ . Structure  $9^+$ , which is accordingly assigned to the  $[\text{bipy}^{\text{Me}},\text{Au},\text{O}_2]^+$  fragment, undergoes subsequent fragmentations. Inter alia neutral  $\text{AuOH}$  can be lost to yield protonated 6-formylbipyridyl ( $11^+$ ,  $[\text{bipy}^{\text{Me}}\text{O} - \text{H}]^+$ ,  $m/z$  185 in Figure 2), or expulsion of water leads to the aldehyde complex  $12^+$ . Note that in both transitions, i.e.,  $9^+ \rightarrow 11^+$  and  $9^+ \rightarrow 12^+$ , the formal gold(III) in compound  $9^+$  is reduced to gold(I). The fragment  $12^+$  can subsequently either undergo decarbonylation to afford  $[(\text{bipy})\text{Au}]^+$  ( $13^+$ ), which corresponds to the overall process of an oxidative dealkylation of  $\text{bipy}^{\text{Me}}$ , or lose neutral  $\text{AuH}$  to afford the acylium ion  $14^+$  followed by the arylum ion  $15^+$  as the quasi-terminal fragment of the sequence. Further, the formation of intermediates bearing a formyl substituent, e.g.,  $12^+$ , also accounts for the loss of  $\text{HCO}^+$  in Figure 4.

#### Infrared Multiphoton Dissociation Spectra of $1^{2+}$ and $2^{2+}$ .

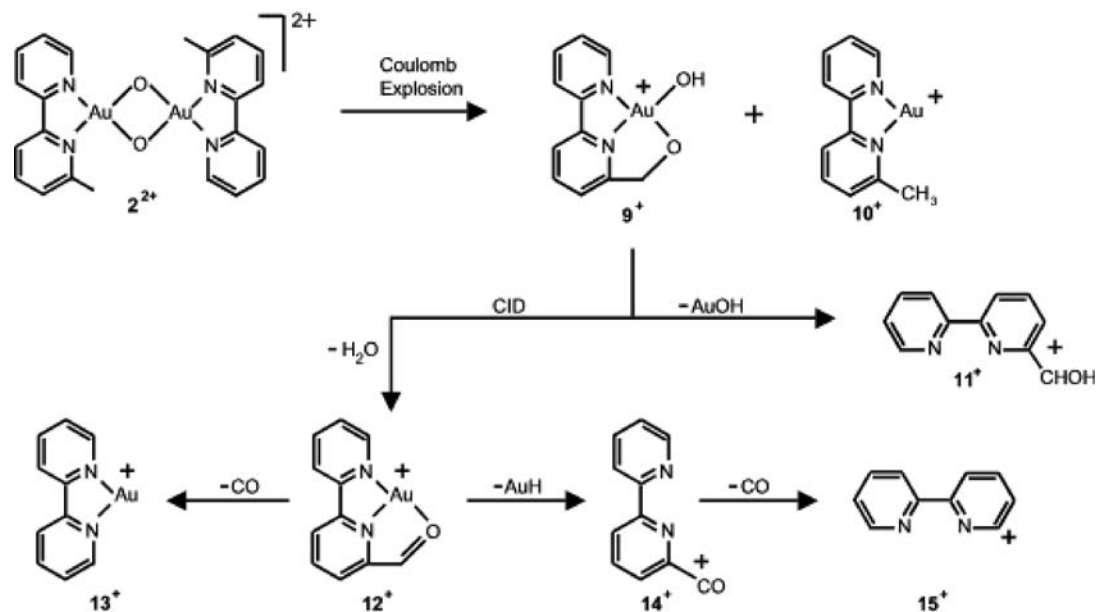
Given the occurrence of C–H bond activation of the  $\text{bipy}^{\text{R}}$  ligands, the question evolves of whether the transfer of the ions from the solution, in which they are stabilized by both solvation and counterions, to the gaseous phase really left them as intact entities. Alternative structural rearrangements, such as bond activations, may have already taken place prior to collisional activation of the precursor ions. Specifically, despite ESI being a soft ionization method, for reactive transition-metal complexes we have previously observed rearrangements occurring in the ion source.<sup>28,51</sup> In this respect we point out that the usually made assumption that ESI leads to a transfer of the intact species of interest into the gas phase once a quasi-molecular ion is seen is not a priori justified, but instead it has to be ensured by independent means. In this respect, the fragmentation behavior of the ion is not a good criterion, because ion fragmentation itself is an energetic process usually associated with structural reorganizations. Reactivity studies are one possibility to determine the actual ion structures,<sup>51</sup> but also these do provide only indirect structural insight. In the specific case studied here, i.e., the large effect of a small substitution, isomerizations occurring in the course of the ionization process may in fact account for most of the observed difference between  $1^{2+}$  and its alkylated derivatives  $2^{2+}$ – $6^{2+}$ . Use of a more direct structural tool is therefore of considerable importance, and for this purpose we employed the IRMPD technique (IRMPD = infrared multiphoton dissociation), which permits the recording of infrared spectra for mass-selected ions in the gas phase.<sup>52</sup>

Figure 5a shows the experimental IRMPD spectrum of mass-selected  $1^{2+}$  (red) with the spectrum of the solid bis(hexafluorophosphate) in the condensed phase (blue) and the computed spectrum of the gaseous ion (green) for comparison; due to the multiphotonic nature of IRMPD experiments, key attention should focus on the band positions rather than signal heights.<sup>40</sup> The generally good agreement between the three spectra provides confirmation that the dication  $1^{2+}$  is transferred intact to the gas phase during the course of electrospray ionization.

- (51) (a) Schröder, D.; Holthausen, M. C.; Schwarz, H. *J. Phys. Chem. B* **2004**, *108*, 14407. (b) Schröder, D.; Schwarz, H.; Aliaga-Alcalde, N.; Neese, F. *Eur. J. Inorg. Chem.* **2007**, 816. (c) Schlangen, M.; Neugebauer, J.; Reiher, M.; Schröder, D.; Pitarch López, J.; Haryono, M.; Heinemann, F. W.; Grohmann, A.; Schwarz, H. *J. Am. Chem. Soc.* **2008**, *130*, 4285. (d) Boyd, J. P.; Schlangen, M.; Grohmann, A.; Schwarz, H. *Helv. Chim. Acta* **2008**, *91*, 1430.
- (52) (a) Dopfer, O. *J. Phys. Org. Chem.* **2006**, *19*, 540. (b) Polfer, N. C.; Oomens, J. *Phys. Chem. Chem. Phys.* **2006**, *9*, 3804.



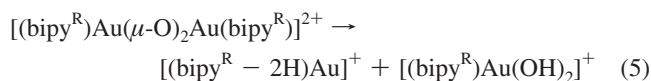
**Scheme 3.** Proposed Fragmentation Sequence of the Dication  $2^{2+}$  To Afford the Monocations  $9^+$  and  $10^+$  as Well as the Subsequent Dissociation Reactions of  $9^+$



Dication  $2^{2+}$  has two isomers with the methyl groups being either *cis* or *trans* with respect to the gold atoms.<sup>14d</sup> At the given level of theory, the *trans*- $2^{2+}$  isomer lies only 2 kJ/mol lower in energy than the *cis* isomer; therefore, the simulated IR spectrum in Figure 5b is given as an average of both spectra. The experimental IRMPD spectrum of mass-selected  $2^{2+}$  (red) in Figure 5b is in reasonable agreement with the spectrum of the solid bis(hexafluorophosphate)s in the condensed phase (blue) and the averaged computed spectrum of the gaseous ion (green). Therefore, we conclude that  $2^{2+}$  is also transferred to the gas phase without the occurrence of rearrangements and the C–H bond activations discussed above thus only occur upon CID.

**Higher Homologues  $3^{2+}$ – $6^{2+}$ .** The fragmentation reactions of the other 6-substituted compounds show a behavior generally similar to that of  $2^{2+}$ . Thus, of all samples investigated in this work, the parent compound  $1^{2+}$  is an exception in that it undergoes dehydration with retention of the 2-fold charge on the ionic fragment, whereas Coulomb explosion is preferred for the other dications. An additional, rather important fragmentation reaction observed for  $3^{2+}$ – $5^{2+}$  is due to Coulomb explosion in

which both oxygen atoms are retained by one fragment with a concomitant transfer of two hydrogen atoms to the oxygen-containing ion fragment from the second ion fragment (reaction 5).



With respect to the ionic products of reaction 5, the structure of the hydrogen-depleted ion  $[(\text{bipy}^R - 2\text{H})\text{Au}]^+$  is not known, but the occurrence of reaction 5 only for the complexes with larger substituents on the bipy ligand indicates an active participation of the side chain.<sup>53</sup> As for the oxygen-containing fragment, the location of the extra hydrogen atoms is unknown: both a gold(III) dihydroxide,  $[(\text{bipy}^R)\text{Au}(\text{OH})_2]^+$ , and a gold oxo aquo complex,  $[(\text{bipy}^R)\text{Au}(\text{O})(\text{H}_2\text{O})]^+$ , are plausible.<sup>54</sup> In fact, CID of mass-selected  $[(\text{bipy}^R)\text{Au}(\text{OH})_2]^+$  shows loss of water as a major fragmentation pathway.<sup>55</sup> Irrespective of the precise ion structure, formation of water would result from a self-sacrificial catalyst in which the desired oxidation process does not occur; thus, complexes which transfer water will most

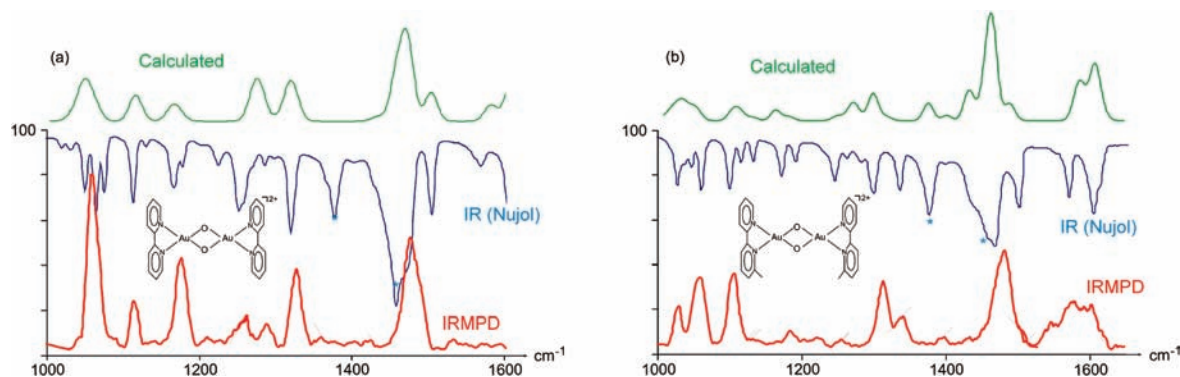


**Figure 5.** Infrared patterns of (a)  $[(\text{bipy})\text{Au}(\mu\text{-O})_2\text{Au}(\text{bipy})]^{2+}$  ( $1^{2+}$ ) in the fingerprint region from 1000 to 1600  $\text{cm}^{-1}$  and (b)  $[(\text{bipy}^{\text{Me}})\text{Au}(\mu\text{-O})_2\text{Au}(\text{bipy}^{\text{Me}})]^{2+}$  ( $2^{2+}$ ) from 1000 to 1650  $\text{cm}^{-1}$ . The experimental IRMPD spectra of the mass-selected ions (red) are shown in comparison with the IR spectra of the solid bis(hexafluorophosphate)s in the condensed phase (blue) and the calculated IR spectra of the free dications (green). The peaks at 1377  $\text{cm}^{-1}$  and the shoulders at about 1460  $\text{cm}^{-1}$  in the condensed-phase IR spectra stem from the embedding Nujol.

likely not be effective oxidizers. The difference in primary fragmentation routes between compound  $1^{2+}$  and compounds  $2^{2+}$ – $6^{2+}$  (Table 1) gives insight toward the effect substituents have on the strength of the complex's backbone. An even more drastic effect of the ancillary ligands' substituents on the reactivity has been observed for most copper(III) oxo-bridged complexes.<sup>13a–d,i,16</sup> Further understanding can be gained by comparing the energy at which fragmentation begins as well as the ratio between fragmentation paths for each complex. Three types of semiquantitative information that can be gathered from CID analysis and have been included in Table 1 are the phenomenological AEs of the fragmentations, the collision energies at which half of the fragmentation has occurred ( $E_{1/2}$ ), and the branching ratios between the various fragments. In addition to the metal-containing fragments discussed so far, the CID spectra also show a series of signals at lower masses that are due to organic cations formed upon detachment of the bipyridine ligand from gold while carrying with it a charge. These bipyridine fragments are seen for complexes  $2^{2+}$ – $6^{2+}$  but differ greatly in abundance for each complex, and in addition to the molecular ions  $[\text{bipy}^R]^+$ , other typical fragments are observed, e.g.,  $[\text{bipy}^R - \text{H}]^+$  and  $[\text{bipy}^R - \text{CH}_3]^+$ ; in Table 1, these fragments are all summed up in the column for  $[\text{bipy}^R]^+$ . Likewise, the various product ions due to incorporation of an oxygen atom into the ligand framework are summed up and denoted as  $[\text{bipy}^R\text{O}]^+$  in Table 1. The abundance of the bipy fragments is relatively small in the spectrum of complex  $2^{2+}$  (Figure 2), whereas other complexes containing organic substituents lead to moderate or even considerable amounts of these organic fragment ions (Table 1).

The major fragment produced upon CID of complex  $4^{2+}$  (containing neopentyl substituents) is a monocation formed upon charge separation concomitant with transfer of two hydrogen atoms and one oxygen atom from one ion fragment to the other (reaction 5). In addition, complex  $4^{2+}$  undergoes Coulomb explosion concomitant with oxygen atom transfer according to reaction 2. Organic ions derived from the bipyridine fragments as well as oxidized fragments are also detected in quantities greater than those seen for complex  $2^{2+}$ . The appearance of oxidized bipyridine fragments and the transfer of water between Coulomb explosion fragments both indicate complex  $4^{2+}$  is likely to be a self-sacrificial catalyst and is not an effective oxidation catalyst.

Compound  $3^{2+}$  consists of the basic  $[(\text{bipy}^R)\text{Au}(\mu\text{-O})_2\text{Au}(\text{bipy}^R)]$  structure with isopropyl groups attached at the 6-position of each bipyridine. The substituents on this complex are not as bulky as the neopentyl groups of complex  $4^{2+}$ , yet

are larger than the methyl groups of complex  $2^{2+}$ , leading us to believe the fragmentation spectrum will be a mixture of those found for complexes  $2^{2+}$  and  $4^{2+}$ . As expected, the major fragment in the CID spectrum comes from the splitting of the compound and transfer of oxygen, while there is also a large quantity of ions resulting from the transfer of water during Coulomb explosion. This result further supports the claim that introduction of large substituents at the 6-position of 2,2'-bipyridine causes self-sacrificial oxidation. It should be noted that the quantities of ionized bipyridine and its oxygenated form are larger than those observed for  $2^{2+}$ , which also appears to be a fragmentation pattern that results from bulky substituents. Additionally, the dication  $3^{2+}$  bears the lowest fragmentation threshold of all compounds studied in this work, and likely it will undergo decomposition more easily than initiating oxygen atom transfer to other substrates.

The CID of dicationic  $5^{2+}$  is unique because the greatest quantities of bipyridine ions and oxidized bipyridine fragments are found. Most likely, the bulky phenyl substituents of  $5^{2+}$  are responsible for the unique fragmentation observed, because greater quantities of charged bipyridine and bipyridine oxide fragments are being created when larger substituents are attached; in the specific case of  $5^{2+}$ , also the formation of annellated heterocycles appears as a feasible option. Complex  $5^{2+}$  is continuing with the trend earlier noted that all substituted bipyridine complexes fragment through Coulomb explosion and has a substantial amount of fragment related to transfer of oxygen in accordance with reaction 2. The weakest bond within the dication  $5^{2+}$  appears to be the Au–N linkage due to the greatest quantity of fragments being bipyridine; oxidation is a competing mechanism with higher energetic demands.

The CID spectrum of  $6^{2+}$  is similar to that of  $2^{2+}$ , which is consistent with the presence of methyl substituents in both dications;  $6^{2+}$  differs by an additional methyl group attached to the 6'-position of each bipyridine. As was detected for complex  $2^{2+}$ , the majority of the fragments are monocations in which one fragment carries both oxygen atoms after cluster cleavage during Coulomb explosion. There are no fragments in which water has been transferred upon Coulomb explosion, and the quantities of bipyridine and bipyridine oxide fragments are minor.

The energetic information gained through CID becomes important, having found two complexes that are both selective toward fragmentation by Coulomb explosion and solely involve oxygen transfer. The phenomenological AEs as well as the corresponding values of  $E_{1/2}$  are given in Table 1 for all compounds. Interestingly, the AE (1.7 eV) for complex  $6^{2+}$  is significantly lower than that of  $2^{2+}$  (2.3 eV), thus supporting the notion that there is more strain on the bonding of the Au–O backbone in complex  $6^{2+}$ . An additional methyl group in each bipyridine ligand of complex  $6^{2+}$  causes a further lengthening of the bonds in the backbone with respect to complex  $2^{2+}$ , which is in good agreement with the geometrical parameters as well as the oxidizing power.<sup>14d</sup> This complex is an attractive candidate for further study, and future complexes should be developed having substituents in both the 6- and 6'-positions to optimize strain in the backbone of the complex.

Even without performance of isotopic labeling experiments, the complete survey of the fragmentation reactions of compounds  $1^{2+}$ – $6^{2+}$  suggests some trends with respect to the location of the C–H bond activation reactions occurring upon CID. Thus, the parent compound  $1^{2+}$  has by far the largest fragmentation threshold of all compounds studied (the formal

(53) Schwarz, H. *Acc. Chem. Res.* **1989**, *22*, 282. For the 2-fold occurrence of remote C–H and C–C bond activations in different parts of flexible molecules, see: (b) Czekay, G.; Eller, K.; Schröder, D.; Schwarz, H. *Angew. Chem., Int. Ed. Engl.* **1989**, *28*, 1277. (c) Schröder, D.; Schwarz, H. *J. Am. Chem. Soc.* **1990**, *112*, 5947.

(54) For similar tautomerisms between cationic metal dihydroxide and metal oxo/water complexes, see: (a) Schröder, D.; Bärsch, S.; Schwarz, H. *J. Phys. Chem. A* **2000**, *104*, 5101. (b) Vukomanovic, D.; Stone, J. A. *Int. J. Mass Spectrom.* **2000**, *202*, 251. (c) Bärsch, S.; Schröder, D.; Schwarz, H. *Chem.–Eur. J.* **2000**, *6*, 1789. (d) Schröder, D.; Schwarz, H. *Int. J. Mass Spectrom.* **2003**, *227*, 121. (e) Schröder, D.; Souvi, O.; Alikhani, E. *Chem. Phys. Lett.* **2009**, *470*, 162. (f) Reference 49a.

(55) Note that the sequence  $[(\text{bipy}^R)\text{Au}(\mu\text{-O})_2\text{Au}(\text{bipy}^R)]^{2+} \rightarrow [(\text{bipy}^R)\text{Au}(\text{OH})_2]^+ \rightarrow [(\text{bipy}^R)\text{AuO}]^+$  leads to a  $[(\text{bipy}^R)\text{AuO}]^+$  monocation which is isobaric with the precursor ion  $[(\text{bipy}^R)\text{Au}(\mu\text{-O})_2\text{Au}(\text{bipy}^R)]^{2+}$ . However, the isotope pattern of the parent ions (see inset a in Figure 1, for example) rules out the occurrence of such sequential fragmentations in the ion source under the ionization conditions chosen.

AE for H<sub>2</sub>O loss from **1**<sup>2+</sup> amounts to 9.7 eV, Table 1), and the expulsion of neutral H<sub>2</sub>O according to reaction 1 is proposed to involve a rollover mechanism (Scheme 2). Obviously, however, such a rollover of the ligand is both energetically and entropically demanding. Introduction of alkyl substituents at the 6-position of the 2,2'-bipyridine clearly lowers the barrier for charge separation according to reaction 2, and loss of water with maintenance of the double charge hardly can compete further. Obviously, a single methyl group in the 6-position is sufficient to initiate this shift in reactivity. In contrast, the formal water transfer concomitant with charge separation (reaction 5) only occurs for the dications **3**<sup>2+</sup>–**5**<sup>2+</sup>, which bear substituents larger than methyl in the 6-position of the bipyridine ligand. It is accordingly suggested that reaction 5 involves activation of remote C–H bonds located on the alkyl substituents in the crucial step,<sup>53</sup> i.e., the CH<sub>3</sub> units of the isopropyl substituent in **3**<sup>2+</sup>, of the neopentyl substituent in **4**<sup>2+</sup>, and—much less favored—on the phenyl groups in **5**<sup>2+</sup>. Consistent with this line of reasoning, the dissociation thresholds of compounds **3**<sup>2+</sup> and **4**<sup>2+</sup> are much lower than those of the others. The particularly low AE for **3**<sup>2+</sup> can be explained by the possibility of a favorable formal 1,2-dehydrogenation, as similar oxidation reactions have precedence in the chemistry of gaseous metal oxide ions<sup>23,56</sup> and also in the condensed phase.<sup>13</sup>

## Conclusions

As demonstrated by analysis of the fragmentation patterns and infrared data, electrospray ionization permits the transfer of dicationic, binuclear Au<sub>2</sub>O<sub>2</sub> complexes of the type [(bipy<sup>R</sup>)Au(μ-O)<sub>2</sub>Au(bipy<sup>R</sup>)]<sup>2+</sup> into the gas phase as intact dications. Upon collisional activation of the mass-selected dications, rather pronounced substituent effects on the fragmentation patterns become apparent. The parent compound [(bipy)Au(μ-O)<sub>2</sub>

Au(bipy)]<sup>2+</sup> (R = H) undergoes dehydration at the dicationic stage to afford another dicationic fragment, most likely [(bipy – H)Au(μ-O)Au(bipy – H)]<sup>2+</sup> formed via a rollover cyclometalation. In contrast, the [(bipy<sup>R</sup>)Au(μ-O)<sub>2</sub>Au(bipy<sup>R</sup>)]<sup>2+</sup> derivatives with several alkyl or aryl substituents in the 6-position of the bipyridine ligands undergo charge-separation reactions, while the loss of water from the dication is almost completely suppressed. The differences in fragmentation patterns are also reflected by much larger appearance energies for fragmentation of the parent compound [(bipy)Au(μ-O)<sub>2</sub>Au(bipy)]<sup>2+</sup> compared to the substituted derivatives. Analysis of the mass spectrometric data implies that the reason for this pronounced substituent effect is due to an attack on C–H bonds in the substituents which are spatially close to the Au<sub>2</sub>O<sub>2</sub> cores of the binuclear clusters. The occurrence of C–H bond activation reactions and also oxygen incorporation into the ligands are demonstrated directly by the formation of oxygenated organic cations at elevated collision energies. Last but not least, the pronounced ligand effect in the gas-phase fragmentation parallels the large differences in the biological activities of these dinuclear gold(III) compounds.

**Acknowledgment.** This paper is dedicated to Professor Yitzhak Apeloig on the occasion of his 65th birthday. This work was supported by the European Commission (EPITOPES, Project No. 15637), the Grant Agency of the Academy of Sciences of the Czech Republic (Grant KJB400550704), the Grant Agency of the Czech Republic (Grant 203/08/1487), the Czech Academy of Sciences (Grant Z40550506), the Ministry of Education of the Czech Republic (Grants MSM0021620857 and RP MSMT 14/63), and the University of Sassari (Grant FAR 2007). The Prague team thanks Joel Lemaire, Philippe Maitre, and the entire staff of CLIO for kind assistance. E.C.T. appreciates the Institute of International Education (IIE) for a generous stipend of his research visit at the Prague team as well as the Department of Energy, Grant DE-FG02-92ER14258, for partial support. F.C. gratefully acknowledges the Fondazione Banco di Sardegna for a two-year fellowship.

JA902773B

(56) (a) Jackson, T. C.; Jacobson, D. B.; Freiser, B. S. *J. Am. Chem. Soc.* **1984**, *106*, 1252. (b) Ryan, M. F.; Fiedler, A.; Schröder, D.; Schwarz, H. *Organometallics* **1994**, *13*, 4072. (c) Ryan, M. F.; Fiedler, A.; Schröder, D.; Schwarz, H. *J. Am. Chem. Soc.* **1995**, *117*, 2033. (d) Trage, C.; Schröder, D.; Schwarz, H. *Organometallics* **2003**, *22*, 693.